ARMY RESEARCH LABORATORY


# Nonlocal Control of Fracture Propagation in Numerical Simulations

**by Richard C. Becker**

**ARL-MR-842** **March 2013**

## NOTICES

### Disclaimers

The findings in this report are not to be construed as an official Department of the Army position unless so designated by other authorized documents.

Citation of manufacturer's or trade names does not constitute an official endorsement or approval of the use thereof.

Destroy this report when it is no longer needed. Do not return it to the originator.

# Army Research Laboratory
Aberdeen Proving Ground, MD 21005-5069

**ARL-MR-842** **March 2013**


# Nonlocal Control of Fracture Propagation in Numerical Simulations


**Richard C. Becker**
**Weapons and Materials Research Directorate, ARL**

| REPORT DOCUMENTATION PAGE | *Form Approved OMB No. 0704-0188* |
|---|---|



| 1. REPORT DATE *(DD-MM-YYYY)* | 2. REPORT TYPE | 3. DATES COVERED (From - To) |
|---|---|---|
| March 2013 | Final | September 2011–December 2012 |

**4. TITLE AND SUBTITLE**
Nonlocal Control of Fracture Propagation in Numerical Simulations

**5a. CONTRACT NUMBER**

**5b. GRANT NUMBER**

**5c. PROGRAM ELEMENT NUMBER**

**6. AUTHOR(S)**
Richard C. Becker

**5d. PROJECT NUMBER**
FPEC02

**5e. TASK NUMBER**

**5f. WORK UNIT NUMBER**

**7. PERFORMING ORGANIZATION NAME(S) AND ADDRESS(ES)**
U.S. Army Research Laboratory
ATTN: RDRL-WMP-C
Aberdeen Proving Ground, MD 21005-5069

**8. PERFORMING ORGANIZATION REPORT NUMBER**
ARL-MR-842

**9. SPONSORING/MONITORING AGENCY NAME(S) AND ADDRESS(ES)**

**10. SPONSOR/MONITOR'S ACRONYM(S)**

**11. SPONSOR/MONITOR'S REPORT NUMBER(S)**

**12. DISTRIBUTION/AVAILABILITY STATEMENT**
Approved for public release; distribution is unlimited.

**13. SUPPLEMENTARY NOTES**

**14. ABSTRACT**
A nonlocal algorithm is used to control the failure propagation rate in finite element simulations. An extension of the method, which creates smooth gradient fields near the fracture front, is explored as a means for improving the advection of discontinuous fields associated with cracks. The algorithms are evaluated by varying fracture propagation speed and assessing crack size changes with advection.

**15. SUBJECT TERMS**
advection, fracture, nonlocal, crack speed, fracture propagation

| 16. SECURITY CLASSIFICATION OF: | | | 17. LIMITATION OF ABSTRACT | 18. NUMBER OF PAGES | 19a. NAME OF RESPONSIBLE PERSON |
|---|---|---|---|---|---|
| a. REPORT | b. ABSTRACT | c. THIS PAGE | | | Richard C. Becker |
| Unclassified | Unclassified | Unclassified | UU | 18 | 19b. TELEPHONE NUMBER (*Include area code*) 410-278-7980 |

**Standard Form 298 (Rev. 8/98)**
Prescribed by ANSI Std. Z39.18

## Contents

## List of Figures

# 1. Introduction

Accurate simulation of fracture in large-scale applications is hampered by both model and numerical algorithmic deficiencies. These are often coupled. The sophistication of a material model can be limited by available numerical methods, so algorithm improvements are often necessary before failure model improvements can be implemented. A particular algorithmic feature explored in this report is allowing the fracture criterion to evolve based on the state of adjacent material.

It is usually easier to propagate an existing crack than to nucleate a new one, and the crack propagation rate is generally controlled either by crack tip kinetic processes or by stress redistribution at the crack front. Fracture models are traditionally considered to be local, which means that all of the information used to progress the material failure is contained in the close proximity of the material point. While this is accurate if the crack tip is spatially resolved and the effects of the stress singularity are captured at neighboring material points, in typical large-scale analyses, the numerical discretization is comparatively coarse and the appropriate stress and strain concentrations are not generated ahead of the unresolved cracks. Further, in a local model, a numerical quadrature point is unaware that fracture may exist at a neighboring quadrature point.

The goal in this work is to provide information about the existence of fracture to neighboring elements in a finite element code and to adjust the failure criterion accordingly. The approach is similar to the algorithm employed in Lagrangian simulations by Wilkins[1] and more recently by Holmquist and Johnson[2]. The development will be in the context of an Arbitrary Lagrange Eulerian (ALE) finite element code, although the algorithm is applicable to other numerical techniques.

# 2. Approach

The approach is a simple nonlocal scheme in which elements containing fractured material inform their neighboring elements of the earliest time when the fracture may arrive at the neighbor locations. This enables two nonconventional fracture model features: the failure criterion can be changed in the vicinity of a crack, and, through the timing of the criterion change, the fracture propagation rate can be controlled from element to element. While the

[1]Wilkins, M. L. Mechanics of Penetration and Perforation. *Int. J. Engng. Sci.* **1978**, *16*, 793–807.

[2]Holmquist, T. J.; Johnson, G. R. *A Computational Constitutive Model for Glass Subjected to Large Strains, High Strain Rates and High Pressures*; Report No. 18.12544/023; Southwest Research Institute: San Antonio, TX, 2010.

technique is nonlocal, it is implemented in an operator-split approach and is minimally disruptive to the finite element code. The method has many components implemented within the traditional material model evaluations and a nonlocal component that involves resetting a history variable in neighboring elements.

### 2.1 Computations During the Constitutive Model Evaluation

The algorithm is illustrated using simple maximum principal stress failure criteria. There are two distinct failure conditions. One is for propagating failure in elements adjacent to material that has already fractured, $F_{prop}$, and the other is for nucleating failure in regions remote from existing cracks, $F_{nuc}$. Generally, $F_{nuc} > F_{prop}$, and the nucleation threshold can be much higher than the propagation threshold for ceramics and glasses. The active failure criterion is assigned by a Boolean state variable within each element, $A_{crit}$. Failure within the element progresses when the maximum principal stress from an elastic stress update, $\sigma_{Pmax}$, exceeds the stress threshold:

$$\sigma_{Pmax} > F\ (1 - f_{extent}). \tag{1}$$

$F$ represents the threshold from whichever failure criterion is active ($F_{prop}$ or $F_{nuc}$). An extent-of-failure variable $f_{extent}$ is introduced to degrade the threshold strength within the element and control the stress reduction. It is essentially a damage variable, but in this simple demonstration implementation, the elastic properties are not degraded with damage.

The evolution of the failure extent variable within the constitutive model is intended to represent crack propagation across an element. If the crack propagates at a speed $C_{crk}$, the failure extent is updated by

$$df_{extent} = \frac{C_{crk}}{L_{len}}\ dt, \tag{2}$$

where $L_{len}$ is a characteristic element length and $dt$ is the time increment. The failure extent variable is bounded, $0 \leq f_{extent} \leq 1$.

The failure is treated as being isotropic, so there is not a unique way to reduce the stress such that the maximum principal stress satisfies equation 1. Here, the pressure and von Mises equivalent stress at the time of initial failure are saved as history variables $p_{atFail}$ and $\sigma^{vm}_{atFail}$, respectively. If the pressure is tensile (negative) following an elastic stress update, the pressure is reset to satisfy

$$p \geq p_{atFail}(1 - f_{extent}). \tag{3}$$

No pressure adjustment is necessary if the inequality is satisfied after the elastic stress update. If the pressure is compressive, it is not reset. Failed, dense, solid material can support pressure, so degrading a compressive pressure would not be consistent with the physics. The deviatoric components of the stress tensor are reduced by the radial return algorithm, if necessary, such that the von Mises stress satisfies

$$\sigma^{vm} \leq \sigma^{vm}_{atFail}(1 - f_{extent}). \tag{4}$$

As with the pressure, the von Mises stress is not reset if it already satisfies the inequality following the elastic stress update. With the exception of the multiple failure criteria, equations 1–4 are a common means for controlling the failure rate within an element.

The failure criterion is set by Boolean state variable $A_{crit}$. This variable defaults to 1 initially, representing undamaged material with failure criterion $F_{nuc}$. It is initially set to 0 in elements containing significant defects that would fracture at the lower criterion, and set to 0 during the course of the calculation if an existing crack could have propagated into the element. This element-to-element propagation, described in the following section, permits control of the crack speed.

## 2.2 Nonlocal Aspects of the Algorithm

The nonlocal aspect of the model is determining when to alter the failure criterion. Each element is given a state variable $t_{arrival}$, representing the earliest time at which a nearby crack, traveling at the rate $C_{crk}$, could arrive at the element centroid. When the current time in the simulation $t$ meets the condition

$$t > t_{arrival} - \frac{1}{2}\frac{L_{len}}{C_{crk}}. \tag{5}$$

$A_{crit}$ is set to 0, triggering the use of the $F_{prop}$ failure criterion. The subtracted term in equation 5 accounts for the crack arriving at the element perimeter, given that the $t_{arrival}$ variable is the arrival time at the element centroid. The $t_{arrival}$ variable is initially set to a value several times the time it takes a crack to propagate across an element. If failure does not progress in an element during a time step, the $t_{arrival}$ variable in that element is incremented by the time step size. This keeps the arrival time well ahead of the current time to prevent premature switching of the failure criterion. Setting of $A_{crit}$ and the incrementation of $t_{arrival}$ by $dt$ are performed during the constitutive model evaluation.

The time of arrival variable $t_{arrival}$ is subject to a more dramatic reset in one of two ways. First, if the failure extent $f_{extent}$ is zero (indicating that the material has not begun to fracture), and the failure criterion, equation 1, is just met for the first time during the current time step, $t_{arrival}$ is set to the current simulation time plus the time it would take the crack to arrive at the element centroid:

$$t_{arrival} = t - dt + \frac{1}{2}\frac{L_{len}}{C_{crk}}. \tag{6}$$

The adjustment by $dt$ puts the crack inside the element boundary. During this time step, $f_{extent}$ is incremented by equation 2 for consistency with the arrival time. Since $f_{extent}$ is no longer zero, this type of a reset can only occur once for each element. This reset is done in the context of the constitutive model calculation.

The second way $t_{arrival}$ is reset is external to the material model when the code has access to all of the current element history variables. For each element in which $f_{extent} > 0$ (called the "seed" element here), the centroid-to-centroid distance $D_{centroid}$ is calculated to all adjacent elements that have not yet begun to fail, $f_{extent} = 0$. The earliest time for arrival of the crack at the centroid of these undamaged neighbor elements is then set by

$$t_{arrival} = \text{Min}\left(t_{arrival}, t^*_{arrival} + \frac{D_{centroid}}{C_{crk}}\right), \tag{7}$$

where $t^*_{arrival}$ is the arrival time for the "seed" element, which has $f_{extent} > 0$. The minimum in equation 7 is necessary since multiple failed neighbors can reset $t_{arrival}$ independently and the shortest time is desired. The reset is only performed if $f_{extent} = 0$, so the minimum arrival time in an element is not reset in this nonlocal computation if failure has already begun.

A subtle point for the time incrementation of $t_{arrival}$ is that its value is increased by the time step in the constitutive model evaluation if failure does not progress. In other words, the $dt$ increment occurs when failure does not progress even if the material is partially failed, $f_{extent} > 0$. The purpose of $t_{arrival}$ in an element with an existing crack is to monitor the time when the crack would finish traversing the element and enter a neighbor. For a stalled crack, the time the crack would exit the element must be increased. By incrementing $t_{arrival}$ for stalled cracks, the arrival time in all of the surrounding undamaged elements will also increase during the nonlocal $t_{arrival}$ reset.

### 2.3 Efforts to Mitigate Advection Issues

Eulerian or ALE calculations move material across element boundaries. The algorithms are designed for accurate advection of smooth, continuous fields, and applying these same methods to the discrete variables associated with failure models can cause problems. Discrete state variables can change abruptly across element boundaries. Advection algorithms average the state of material entering an element with the state of the remaining material, and the smeared result is often not meaningful for the algorithm. Integer variables like $A_{crit}$ must be either 0 or 1. The advection result may not be proper even for real valued history variables, such as $f_{extent}$. This represents the fractional extent a crack has propagated across an element. It is a decimal value in the element containing the crack tip, and it must be 0 in elements ahead of the crack and 1 in elements behind the crack. It makes no sense to be 0.8 in one element and 0.05 in the neighbor ahead of the crack. Hence, some additional checks and calculations are developed in the attempt to improve the behavior of the model during advection. The following approach is, ultimately, not satisfactory, but it represents some progress in making the advected fields consistent.

The strategy is to develop the midpoint crack arrival time state variable into a longer-range, smooth field that will advect more accurately. Calculations based off of this state variable should be improved. The $t_{arrival}$ variable is propagated spatially by extending the seed elements in calculations using equation 7 to include all elements rather than only elements that have

begun to fail. The $t_{arrival}$ variable in elements adjacent to a fracture is set as previously described, and this serves as the seed for setting $t_{arrival}$ in the next-near neighbor elements and so on. This constructs a smooth, long-range gradient field, and $t_{arrival}$ is still set only in elements that have not yet begun to fracture. That keeps $t_{arrival}$ in actively failing elements near the current time. There is a lag built into the propagation algorithm due to the step-by-step propagation of information. However, the incrementation of $t_{arrival}$ by $dt$ advances an established gradient field uniformly in time, so the lag is evident only where the gradient is being established or modified.

The value of $t_{arrival}$ is capped at several element-to-element propagation times above and below the current time, since the gradients are only needed in the vicinity of the current time. Capping the value at the lower end also circumvents problems where bits of material fractured much earlier in the calculation can contact pristine material through advection and significantly lower the $t_{arrival}$ value.

In Eulerian or ALE codes, there is often the opportunity to adjust the material state variables following advection to bring the material model into a consistent state. During this adjustment, the smooth $t_{arrival}$ values are used to redefine the more step-like $f_{extent}$ value.

$$f_{extent} = \begin{cases} 0 & t_{arrival} > t + \frac{1}{2}\frac{L_{len}}{C_{crk}} - \epsilon \\ 1 & t_{arrival} < t - \frac{1}{2}\frac{L_{len}}{C_{crk}} + \epsilon \\ \frac{1}{2} + (t - t_{arrival})\frac{C_{crk}}{L_{len}} & \text{otherwise} \end{cases} . \quad (8)$$

The $\epsilon$ is a small "fuzz" value intended to keep $f_{extent}$ values above the numerical noise. In the latter case of equation 8, $f_{extent}$ is subsequently checked to ensure that it lies between 0 and 1. A tolerance $\delta$ is placed on this check to truncate results that are close to the bounds. The effect of this tolerance is described at the end of section 3.3.

The fracture model and nonlocal algorithm setting the state variables were implemented in Lawrence Livermore National Laboratory code ALE3D.[3] The nonlocal method is quite similar to element-to-element lighting time algorithms for explosive burn, so much of the infrastructure was already in place. It is anticipated that implementation would be similarly straightforward in other codes with similar features.

[3]Nichols, A. L., Ed. *Users Manual for ALE3D: An Arbitrary Lagrange/Eulerian 2-D and 3-D Code System*; Lawrence Livermore National Laboratory: Livermore, CA, 2009.

## 3. Results

The ability of the model to control the failure propagation rate is illustrated through plane-strain crack growth simulations in which limiting fracture propagation speeds are specified as 2 and 4 mm/μs. The geometry of the brittle target plate is a 100 × 100 mm square with a 20-mm deep crack on the right side, as shown in figure 1. The element size is 0.25 mm in the *x* and *y* directions, in both the plate and the in projectile. The plate is impacted by a 10-mm-wide by 20-mm-long block of steel at 0.1 mm/μs.

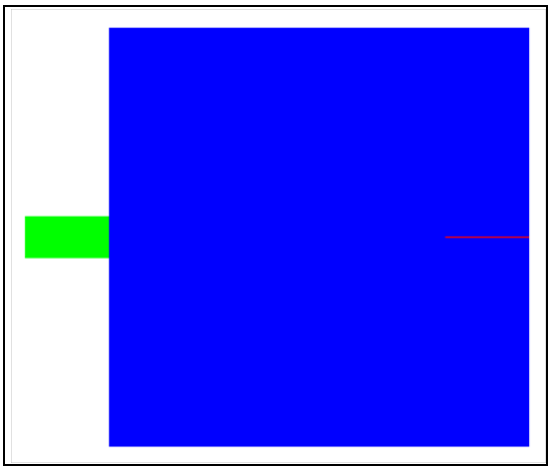

Figure 1. Initial plane-strain configuration showing the target plate, the projectile, and the initial crack at the right side.

The plate has a density of 3.9 $cm^3$ and is modeled with a Murnaghan equation of state with a reference bulk modulus of 228 GPa. The pressure dependence of the bulk modulus is 2.0 and the Gruneisen parameter is set to 2. The shear modulus is 152 GPa. The critical principal stress for fracture nucleation is set to 30 GPa, which is never reached in these simulations. The critical principal stress for propagating existing fractures is set to 200 MPa.

The compressive stress wave initiating at the impact site traverses to the right, where it reflects off of the surface as a tensile wave. The tensile wave interacts with the preexisting crack, and the crack grows. Given the simple nature of the fracture model, the cracks tend to follow the mesh, but some cracks are driven hard enough to run skew to the mesh. The obvious mesh dependence is not important for current purposes, as the goal is to demonstrate control of the fracture propagation rate and the influence of advection on the failure.

### 3.1 Fracture Rate Control

The ability of the algorithm to control fracture rate is illustrated for Lagrangian simulations in figure 2. Figures 2a and 2b show the fracture configuration at 35 and 50 μs, respectively, after impact in simulations with the fracture velocity limited to 2 mm/μs. Given this speed and the time increment between the frames, the most a crack would have been permitted to progress between these two frames is 30 mm, less than one-third of the distance across the plate. Examining the crack propagating to the left in figures 2a and 2b, the distance progressed appears to follow the growth restriction. Figures 2c and 2d show the fracture configuration at the same times, but with a limiting fracture velocity of 4 mm/μs. It is evident that the cracks are growing faster, as permitted.

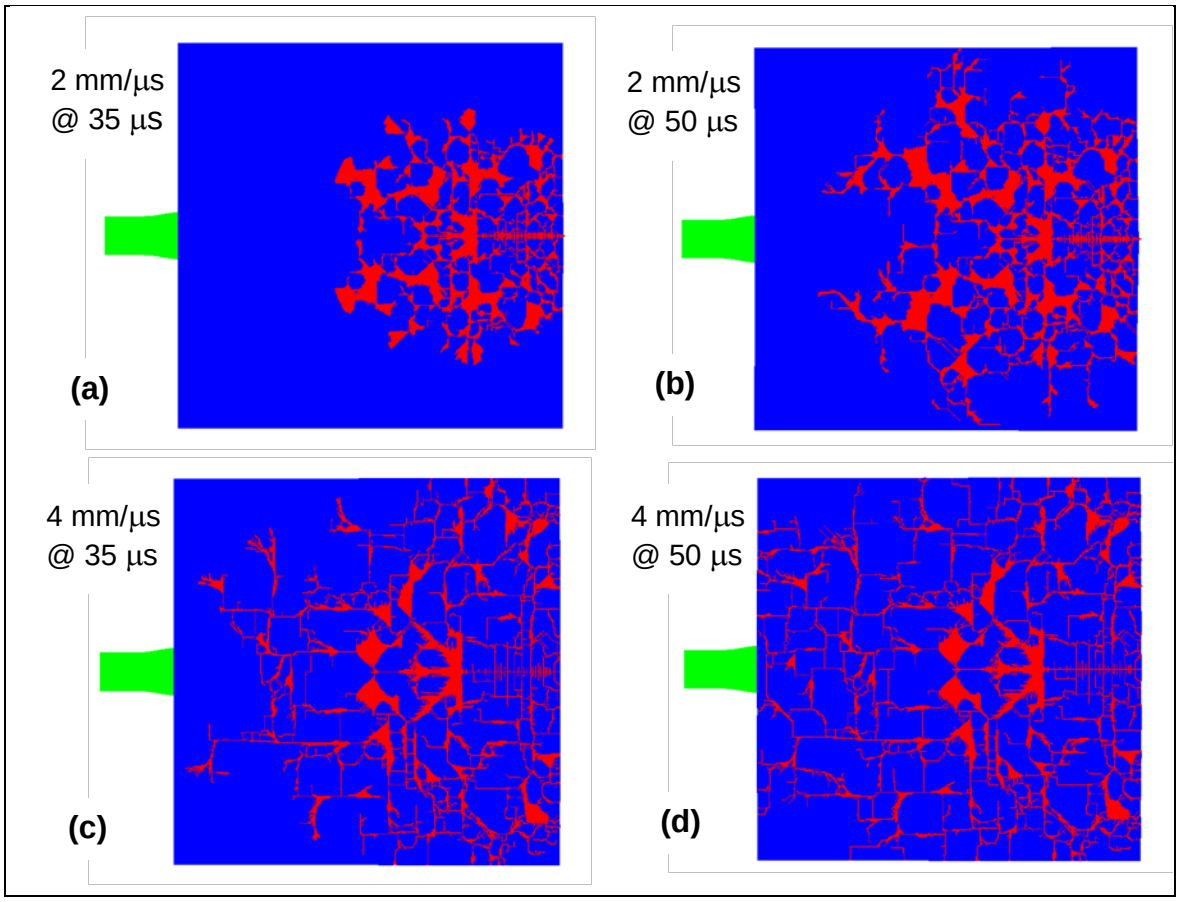


Figure 2. Fracture configurations at 35 and 50 μs for plane-strain simulations with failure propagation rates restricted to 2 and 4 mm/μs.

Note that controlling the failure propagation rate also affects the failure pattern. Overall, the slower propagation rate appears to create more regions where the failure pattern is spread spatially. Also, the cracks do not appear to follow the mesh as readily when the propagation rate is more restricted. When the propagation rate is slower, the stress is not relieved as quickly or

focused as tightly along the mesh lines ahead of the cracks. This provides the crack an opportunity to grow in other directions rather than following the mesh.

In general, the cracks tend to propagate along mesh lines because the failure criterion is reduced along the mesh direction earlier than it is reduced along the diagonal.

### 3.2 Arrival Time Field

The crack arrival time field is depicted in figure 3 for the 4-mm/μs propagation rate calculation. The time is 35 μs, which corresponds to the color cyan in the plots. The zoomed region in figure 3b is taken from the upper left of figure 3a. The plots show that the arrival time field is smooth and continuous for future times. In the narrow areas where the crack is actively extending, the color scale is continuous to times earlier than the present. However, most of the dark blue elements are adjacent to cyan. This color scale discontinuity indicates crack surfaces that have not propagated for the last several time steps. Since the arrival time is updated only with the gradient algorithm in elements with no damage, times in the past do not get set by the gradient algorithm. They are only truncated to keep the time from lagging too far behind the current time.

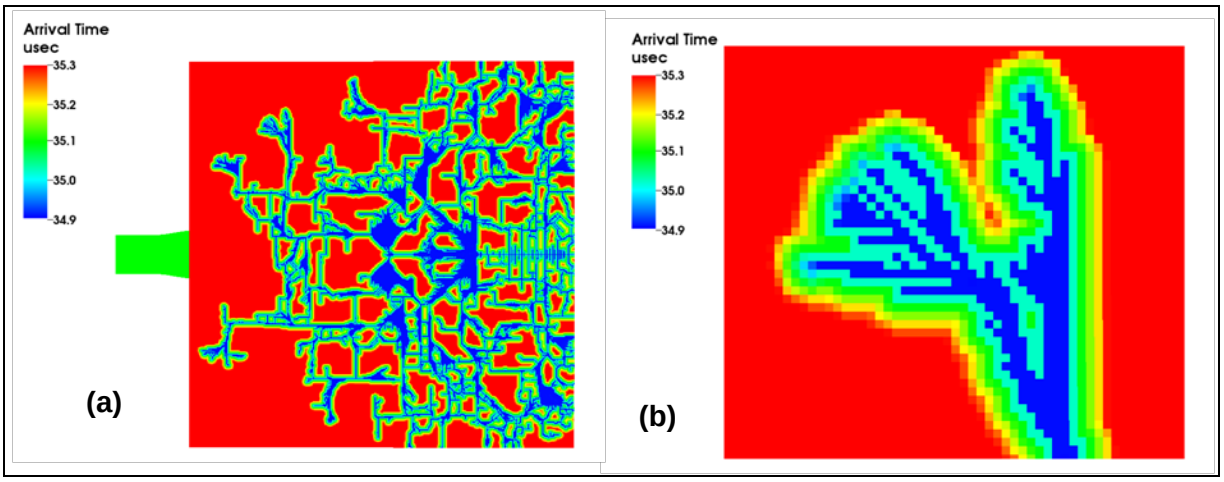


Figure 3. Plot of the earliest possible time of arrival of the fracture at 35 μs for the 4-mm/μs fracture propagation speed: (a) full field and (b) enlargement of active branch near the upper left.

While it would be beneficial to have arrival times continuous into the past to provide smoother fields for advection, attempts to set the previous arrival times in the gradient algorithm created feedback loops that altered the future times as well. Further development in this area is needed.

### 3.3 Advection Effects

The same model geometry is used to evaluate the effects of advection on the solution. For the applications and brittle materials targeted with this model construct, it is anticipated that the deformation and material motion through the mesh will be small prior to fracture and that large

deformation is possible after initial fracture. Fracture patterns from three simulation approaches are shown in figure 4: the first is a pure Lagrangian calculation, the second a Eulerian calculation where the penetrator is moving into an initially stationary target, and the third an Eulerian calculation where the target moves to the left into a stationary rod. The difference between the two Eulerian calculations is the range of motion of the material through the mesh. When the target is initially stationary, much of the fracture occurs before the target begins moving appreciably to the right. When the target is initially moving, the cracks all traverse several elements of the Eulerian mesh.

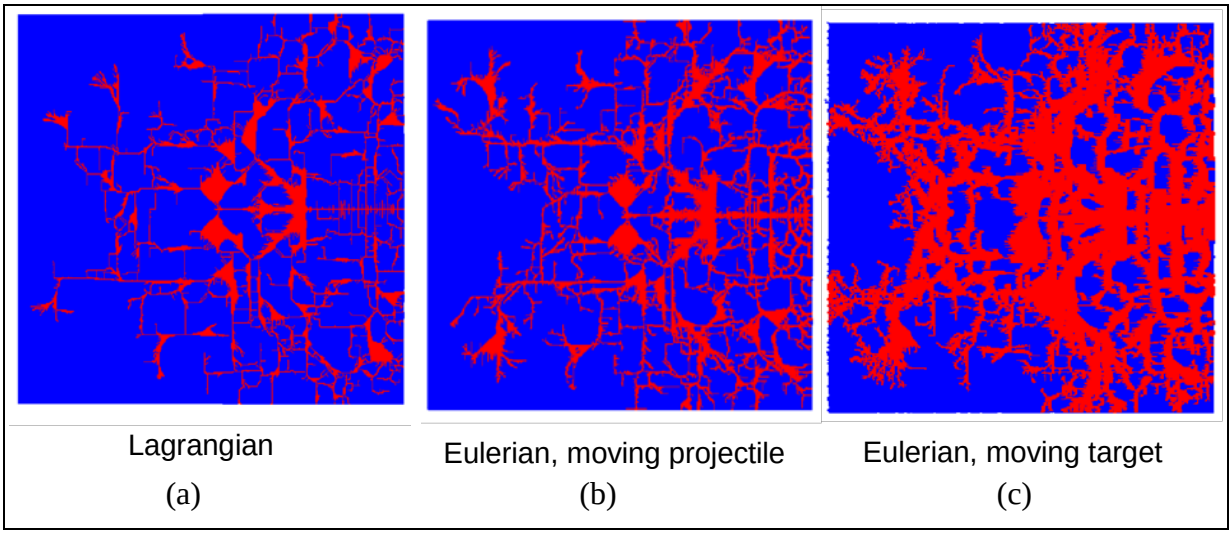


Figure 4. Numerical diffusion of fracture field as a function of extent of advection: (a) Lagrange simulation, no advection; (b) Eulerian with initially stationary target, little advection; and (c) Eulerian with target moving into projectile, significant advection.

Fine cracks, many an element in width, span the Lagrangian target in figure 4a. The cracks maintain their width and location in the target over time, which is consistent with the physics of fractured materials. The fracture pattern is similar in the Eulerian simulation with the initially stationary target, figure 4b. The material is almost Lagrangian because the target starts to accelerate downstream only as the momentum is transferred from the projectile. There is some growth in the width of the vertical cracks as the advection algorithm smears the cracks horizontally. This advection-related crack diffusion is greater on the right side of the plot where cracks formed earlier and have been in motion longer. The cracks also grow wider as the simulation progresses.

The initially moving Eulerian target, figure 4c, shows significant crack diffusion with mesh motion. The algorithm setting the minimum time of arrival in a smooth gradient did not prevent spreading of the discontinuous crack field. Close inspection of the results shows that the arrival time algorithm was partially successful. On the crack flank that is advancing into the mesh (left

side of the vertical cracks in figure 4c), the arrival time gradient moves with the material and the $f_{extent}$ calculated from equation 8 behaves as desired. The extent, representing the location of the crack flank, is between 0 and 1 only in one element at a time, so that the leading edge of the crack flank is tracked as a sharp interface. The error occurs on the trailing crack flank. The minimum in the algorithm setting the crack arrival time continually resets the timing of the gradient, and the gradient stays approximately fixed to the stationary mesh. Hence, the downstream crack flank stays fixed in space due to the calculations in equation 8. This is no better than applying the advection directly to integers.

If the trailing crack flank could be differentiated from the leading flank, the algorithm could be modified to treat the upward gradient in failure times differently, and the trailing edge of the crack would also move through the mesh. While this information exists for upwinding of advected variables, it is not directly available in the data constructs where the nonlocal calculations are performed.

If the tolerance $\delta$, associated with the last of equation 8, is set large compared to the advection of $f_{extent}$ through the mesh, the leading edge of the crack can also be fixed to the mesh rather than moving with the material. Therefore, this value should be kept small enough to remove only the numerical round-off from the computation.

## 4. Summary and Conclusions

A nonlocal algorithm has been described for controlling failure propagation rates in Lagrangian finite element calculations. It is an implementation of a procedure used by Wilkins[1] for ceramics several decades ago and more recently by Holmquist and Johnson.[2] When implemented in a massively parallel finite element code for Lagrangian simulations, the method is successful in controlling fracture propagation rates with minimal computational overhead.

A method was explored to improve advection of fracture in Eulerian and ALE codes by propagating the earliest time of arrival of the crack several elements away from the crack surface. This created a smooth gradient field that would advect more accurately than spatially discontinuous state variables associated with fracture. This technique was marginally successful, and it was determined that it is necessary to treat the leading edge and trailing edge of this gradient field differently. The leading flank of a propagating crack advanced as intended, while the trailing edge did not. These results suggest a path forward, but further research into advection of discontinuous fields is needed. The current method is anticipated to be well suited for materials that become finely comminuted behind the failure front, and accurate representation of discrete cracks is not required.

NO. OF COPIES ORGANIZATION

1 (PDF) DEFENSE TECHNICAL INFORMATION CTR
DTIC OCA
8725 JOHN J KINGMAN RD
STE 0944
FORT BELVOIR VA 22060-6218

1 (HC) DIRECTOR
US ARMY RESEARCH LAB
IMAL HRA
2800 POWDER MILL RD
ADELPHI MD 20783-1197

1 (PDF) DIRECTOR
US ARMY RESEARCH LAB
RDRL CIO LL
2800 POWDER MILL RD
ADELPHI MD 20783-1197

2 (PDF) SANDIA NATL LABS
S SCHUMACHER
E HARSTAD
MS 0836
PO BOX 5800
1515 EUBANK SE
ALBUQUERQUE NM 87185-0836

2 (PDF) SANDIA NATL LABS
J NIEDERHAUS
E STRACK
MS 1323
PO BOX 5800
1515 EUBANK SE
ALBUQUERQUE NM 87185-1323

3 (PDF) LAWRENCE LIVERMORE NATL LABS
R MCCALLEN
A NICHOLS
A ANDERSON
PO BOX 808 L-098
7000 E AVE
LIVERMORE CA 94550

2 (PDF) LAWRENCE LIVERMORE NATL LABS
D FAUX
N BARTON
PO BOX 808 L-140
7000 E AVE
LIVERMORE CA 94550

NO. OF COPIES ORGANIZATION

1 (PDF) US ARMY TANK-AUTOMOTIVE RSRCH DEV & ENGRNG CTR
AMSRD TAR
R RICKERT
MAIL MIL
6501 E 11 MILE RD
WARREN MI 48397-5000

1 (PDF) US ARMY ARDEC
S RECCHIA
RDAR MEF E
BLDG 94
PICATINNY ARSENAL NJ 07806-5000

2 (PDF) NAVSEA DAHLGREN
C DYKA
M HOPSON
6138 NORC AVE STE 313
DAHLGREN VA 22448-517

ABERDEEN PROVING GROUND

16 (PDF) DIR USARL
RDRL WML B
B RICE
RDRL WMM
J BEATTY
RDRL WMM B
G GAZONAS
B LOVE
RDRL WMP
S SCHOENFELD
RDRL WMP B
S SATAPATHY
RDRL WMP C
R BECKER
S BILYK
T BJERKE
J CLAYTON
B LEAVY
RDRL WMP D
R DONEY
D KLEPONIS
H MEYER
S SCHRAML
G VUNNI

INTENTIONALLY LEFT BLANK.